ACS APPLIED MATERIALS & INTERFACES

Research Article

www.acsami.org

Superb Adsorption Capacity and Mechanism of Flowerlike Magnesium Oxide Nanostructures for Lead and Cadmium Ions

Chang-Yan Cao, Jin Qu, Fang Wei, Hua Liu, and Wei-Guo Song*

Beijing National Laboratory for Molecular Science, Laboratory of Molecular Nanostructures and Nanotechnology, Institute of Chemistry, Chinese Academy of Sciences, Beijing 100190

Supporting Information

ABSTRACT: A facile method based on microwave-assisted solvothermal process has been developed to synthesize flowerlike MgO precursors, which were then transformed to MgO by simple calcinations. All the chemicals used (magnesium nitrate, urea, and ethanol) were low cost and environmentally benign. The products were characterized by X-ray powder diffraction, scanning electron microscopy, transmission electron microscopy, high-resolution TEM, and N_2 adsorption-desorption methods. These flowerlike MgO nanostructures had high surface area and showed superb adsorption properties for Pb(II) and Cd(II), with maximum capacities of 1980 mg/g and 1500 mg/g, respectively. All these values are significantly higher than those reported on other nanomaterials. A new adsorption mechanism involving solid−liquid interfacial cation exchange between magnesium and lead or cadmium cations was proposed and confirmed.

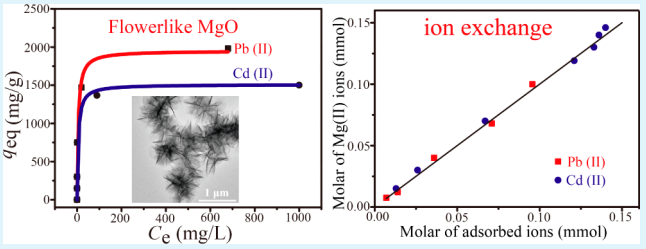

KEYWORDS: *flowerlike, magnesium oxide, nanostructure, heavy metal ion, adsorption, ion exchange*

1. INTRODUCTION

Heavy metal ions, such as Pb(II), Cd(II), and Hg (II), are highly toxic water pollutants, which can have serious side effects and toxicities with a few being lethal and carcinogenic when their concentrations are higher than permissible limits. Therefore, their efficient removal from water is of great importance. Among all the removal methods, the adsorption technique is perhaps the most extensively adopted one because of its low cost and simplicity.[1−16] However, traditional absorbents such as activated carbon, activated alumina, clay, zeolite, etc., show limited adsorption abilities for these heavy metal ions.[17] In recent years, using metal oxide or metal hydroxide nanomaterials for heavy metal ions removal has attracted much attention because of their low cost, environmentally benign nature, and excellent adsorption properties.[8,13,18−20] In particular, three-dimensional (3D) flowerlike metal oxides that are composed of nanometer-sized building blocks with the total size in the micrometer scale have many advantages in adsorption.[2,3,21] Their nanometer-sized building blocks provide high surface area and active sites for adsorption and the overall micrometer-sized structure provides desirable mechanical strength and easy recovery.

The most common synthesis method for flowerlike nanostructures is ethylene glycol (EG)-mediated process.[3,5,22,23] For example, in our previous study, flowerlike MgO nanostructures were prepared through heating magnesium acetate and urea in EG at 180 °C for 5 h, using poly(vinylpyrrolidone) (PVP) as surfactants, followed by calcination.[7] However, this synthesis method for flowerlike MgO nanostructures is not suitable for practical applications because it consumes EG and PVP, making it difficult to use them in practical water purification. Therefore, it is very desirable to develop a low-cost and efficient way to produce flowerlike MgO nanostructures.

As the pH of zero point for MgO aqueous solution is 12.4, it is usually used as adsorbent for heavy metal anion because of electrostatic attraction.[18] Thus, most studies reported in the literatures focus on investigating the adsorption properties of MgO nanomaterials for anions, such as arsenates. The study of MgO for adsorption of cations is rare. Understanding the adsorption mechanism of MgO for heavy metal ions is important for rational design and fabrication of useful adsorbents. In general, as a solid-liquid interfacial process, the adsorption of ions on adsorbents is initialized by electrostatic attraction and may also followed by ion exchange, which usually occurs between the surface hydroxyl groups and the anions (such as arsenate ions).[18,21,24] However, what species are involved in the adsorption process of heavy metal cations has not been elucidated.

In this study, we develop a facile and low-cost method to prepare flowerlike MgO nanostructures via microwave assisted solvothermal method. All chemicals (magnesium nitrate, urea and ethanol) used are low cost and environmentally benign. These flowerlike MgO nanostructures show superb adsorption properties for heavy metal cations, with maximum adsorption capacities of 1980 and 1500 mg/g for Pb(II) and Cd(II),

Received: May 31, 2012
Accepted: July 19, 2012
Published: July 19, 2012

 © 2012 American Chemical Society dx.doi.org/10.1021/am300972z | ACS Appl. Mater. Interfaces 2012, 4, 4283−4287

respectively. In particular, 1 g of flowerlike MgO nanostructures could purify about 630 kg of Pb(II) or 400 kg of Cd(II) contaminated water, reducing the concentration from 200 μg/L to less than 10 μg/L. A new adsorption mechanism involving solid−liquid interfacial cation exchange between magnesium and lead or cadmium cations is proposed and confirmed.

2. EXPERIMENTAL SECTION

Preparation of Flowerlike MgO Nanostructures. All the materials, including magnesium(II) nitrate hexahydrate ($Mg(NO_3)_2{\cdot}6H_2O$), urea, and ethanol, were used as purchased from Beijing Chemicals Co. (Beijing, China). In a typical procedure, 5 mmol of $Mg(NO_3)_3{\cdot}6H_2O$ and 10 mmol of urea were dissolved in 100 mL of ethanol, and then 30 mL of the reaction solution was poured into a Teflon-lined autoclave with volume of 70 mL. The autoclave was sealed and placed in a programmable microwave oven (MDS-6, Shanghai Sineo Microwave Chemistry Technology Co., Ltd.). The oven was heated to 150 °C in 3 min by microwave irradiation and then kept at that temperature for 30 min. After cooling to room temperature, precipitate was collected as MgO precursors by centrifugation and washed with ethanol and water for several times. Flowerlike MgO was obtained by calcinations of the precursors in air at 400 °C for 2 h.

Characterizations. X-ray diffraction (XRD) patterns were obtained with a Rigaku D/max-2500 diffractometer with Cu Kα radiation (λ = 1.5418 Å) at 40 kV and 100 mA. The microscopic features of the samples were characterized by field-emission scanning electron microscopy (FESEM, JOEL 6701F), transmission electron microscopy (TEM, JEOL 1011) and high-resolution transmission electron microscopy (HR-TEM) (FEI Tecnai F20). The nitrogen adsorption and desorption isotherms were measured on a Quantachrome Autosorb AS-1 instrument.

Heavy Metal Ion Adsorption. Solutions with different concentrations of Pb(II) and Cd(II) were prepared using lead nitrate and cadmium nitrate as the sources of heavy metal ions, respectively. The pH value was adjusted to 7. For the adsorption kinetic study, 10 mg of flowerlike MgO nanostructures were added to 15 mL solutions with an initial concentration of 100 mg/L. After a specified time, the solid and liquid were separated immediately and analyzed by inductively coupled plasma−optical emission spectroscopy (Shimazu ICPE-9000) to measure the concentration of metal ions in the remaining solution. For the adsorption isothermal study, 10 mg of adsorbent was added to 15 mL solution with different concentrations under stirring for 12 h at room temperature. The adsorption data were fitted with the Langmuir model as follows

$$q_e = q_m b C_e/(1 + bC_e)$$

Where C_e is the equilibrium concentration of heavy metal ions (mg/L), q_e is the amount of heavy metal ions adsorbed per unit weight of the adsorbent at equilibrium (mg/g), q_m (mg/g) is the maximum adsorption capacity and b is the equilibrium constant related to the adsorption energy.

For adsorption at low concentration, 5 mg of the adsorbent was added to different volumes of heavy metal ion solution with an initial concentration of 200 μg/L.

3. RESULTS AND DISCUSSION

3.1. Characterizations of Flowerlike MgO Nanostructures. Flowerlike MgO nanostructures are prepared via microwave assisted solvothermal method, which is a facile and efficient way for synthesis of different kinds of nanomaterials. In recent studies, flowerlike α-Fe_2O_3 nanospheres,[21] flowerlike NiO hollow nanospheres,[25] and CeO_2 hollow nanospheres[26] were prepared via this microwave assisted thermal method. The microwave heating is fast and spatially uniform. With magnesium nitrate and urea as raw materials and ethanol as solvent, flowerlike MgO precursors can be prepared, followed by mild calcination to obtain flowerlike MgO nanostructures.

Figure. 1a shows the SEM image of the as-prepared MgO precursors, which reveal many flowerlike structures with an

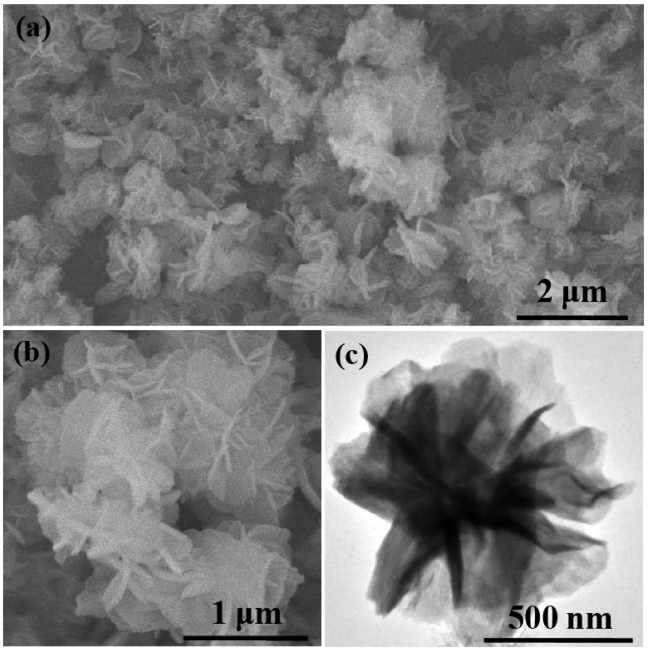

Figure 1. (a) Low-magnification SEM image, (b) high-magnification SEM image, and (c) TEM image of the as-prepared flowerlike MgO precursors.

average diamater of ca. 1 μm. High-magnification SEM image of the sample (Figure 1b) indicates that the flowerlike MgO precursor is composed of twisted nanosheets as the building blocks. TEM image (Figure 1c) further confirms the flowerlike morphology of MgO precursor. XRD result (Figure 2a) shows

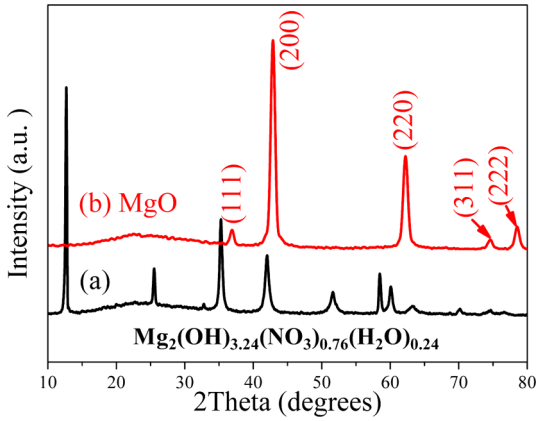

Figure 2. XRD patterns of (a) as-prepared flowerlike MgO precursors and (b) flowerlike MgO nanostructures.

that all diffraction peaks can be indexed to $Mg_2(OH)_{3.24}(NO_3)_{0.76}(H_2O)_{0.24}$ (JCPDS 47-0436). After calcination at 400 °C for 2h in air, the precursors are transformed to pure phase MgO. The XRD pattern of calcined product (Figure 2b) matches well with the stadard PDF card (JCPDS 75-0447).

SEM and TEM images (Figure 3a, b) show that morphology of obtained flowerlike MgO is very similar to that of precursors,

dx.doi.org/10.1021/am300972z | ACS Appl. Mater. Interfaces 2012, 4, 4283−4287

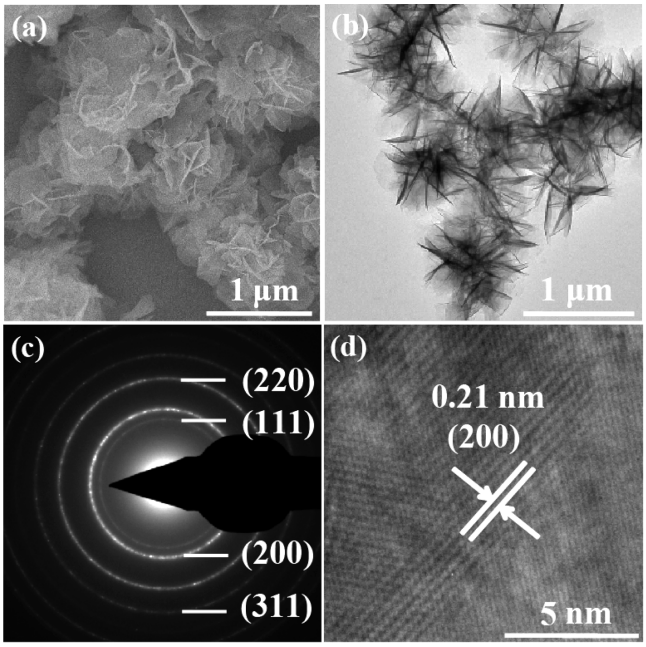

Figure 3. (a) Low-magnification TEM image, (b) high-magnification TEM image, (c) SAED pattern, and (d) HR-TEM image of flowerlike MgO nanostructures.

indicating that calcination does not change the total morphology of MgO. The SAED pattern (Figure 3c) shows bright circled rings, indicating polycrystalline nature of flowerlike MgO. The high-resolution TEM (HR-TEM) image is shown in Figure 3d. The lattice fringes are clearly visible with a spacing of 0.21 nm, corresponding to the spaces of the (200) planes of MgO. The BET surface area of flowerlike MgO measured from nitrogen adsorption-desorption isotherms is 72 m^2/g (see Figure S1 in the Supporting Information).

3.2. Heavy Metal Ion Adsorption Property. Lead and cadmium are two of the most toxic heavy metal cation ions in drinking water resource, and their efficient removal is critical for safe drinking water. The ability of flowerlike MgO nanostructures as absorbents for heavy metal ion removal was tested. Figure 4a shows the adsorption rates of Pb(II) and Cd(II) ions with initial concentration of 100 mg/L using the flowerlike MgO nanostructure sample. The adsorption processes are very fast during the first 30 min, and the equiribria are established after 1 h. To further investigate the adsorption property, we obtained adsorption isothermswith different initial concentrations ranging from 100 to 5000 mg/L, as shown in Figure 4b. The adsorption data agree well with Langmuir model, indicating a surface adsorption process for these two cations. The maximuim adsorption capacities are 1980 and 1500 mg/g for Pb(II) and Cd(II), respectively. These two values are likely the highest among the adsorption data reported in the literatures, and are significantly higher than those of many reported nanomaterials, as shown in Table 1. Note that the maximum adsorption capacities of other materials in Table 1 are usually measured with optimal pH value. For example, the pH value was ajusted to promote better performance of the adsorbents. In this study, the pH value of test water was about 7.

Table 1. Maximum Adsorption Capacities of Different Adsorbents for Pb(II) and Cd(II)

adsorbents	surface area (m^2/g)	adsorption capacity (mg/g) Pb(II)	adsorption capacity (mg/g) Cd(II)	pH
flowerlike MgO (this study)	**72**	**1980**	**1500**	**7**
magnesium silicate hollow nanospheres[27]	531	300		7
appapulgite clay@carbon nanocomposite[28]	61.8	263.8		6
flowerlike zinc silicate[29]	236	210		7
flowerlike γ-AlOOH nanostructure[30]	145.5	124.2		7
chrysanthemum-like α-FeOOH[9]	120.8	103		7
Zn_2GeO_4-EDTA hybrid membrane[31]		74.6		
urchinlike Ni−P microstructure[32]	425	39	40.7	

For pratical water purification, the Pb(II) or Cd(II) concentration in contaminated drinking water supply is usually less than 200 μg/L. Thus the removal capacity at low concentration is more important for adsorption materials. In a series of experiments, we fix the weight of flowerlike MgO nnaostructures at 5 mg and the initial concentration of Pb(II) or Cd(II) at 200 μg/L with pH values of 7, then varied the volume of the Pb II) or Cd(II) solutions from 0.5 to 4 L. The

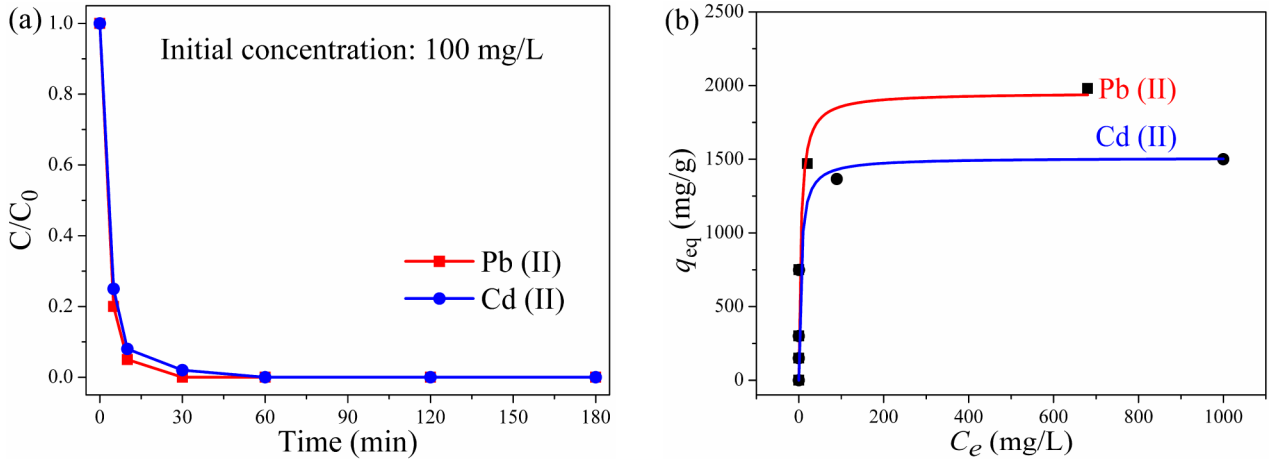

Figure 4. (a) Adsorption rates and (b) adsorption isotherms of Pb(II) and Cd(II) with flowerlike MgO nanostructures as adsorbents.

dx.doi.org/10.1021/am300972z | ACS Appl. Mater. Interfaces 2012, 4, 4283−4287

results are depicted in Figure 5 and Table S1 in the Supporting Information. The breakthrough point (defined as concentration

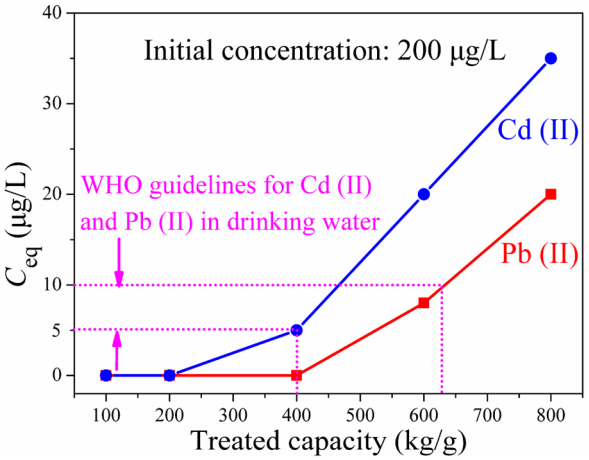

Figure 5. Treatment capacity of flowerlike MgO nanostructures for Pb(II) and Cd(II) with initial concentrations at 200 μg/L.

limit set by the World Health Organization for drinking water, i.e., 10 μg/L for Pb(II) and 5 μg/L for Cd(II), respectively) of the MgO was measured against Pb(II) and Cd(II). Apparently, 5 mg of flowerlike MgO nnaostructures can purify about 3 L of water containing Pb(II) or 2 L of water containing Cd(II) with initial concentration of 200 μg/L before the breakthrough point is reached. Those data suggest that 1 g of flowerlike MgO nnaostructures is able to treat about 630 kg of Pb(II) contaminated water or 400 kg of Cd(II) contaminated water with a pH value of 7, as shown in Figure. 5.

3.3. Adsorption Mechanism. In general, heavy metal ions are adsorbed on metal oxide nanomaterials through electrostatic or/and ion exchange. Surface hydroxyl groups are mainly reported to be involved in the ion exchange process during anion adsorption.[21,24] However, such ion exchange mechanism does not work for cation adsorption because cations and hydroxyl groups have the opposite electric charge. Thus we envision that Mg (II) may be involved in the adsorption. The Mg (II) concentrations after each adsorption of heavy metal ions are tested and the results are list in Table S2. It is very interesting to find that magnesium ions appear in the solution after adsorption and the concentration increases with the increases of adsorption capacity. This result indicates that magnesium ions have exchanged with Pb(II) or Cd(II) during adsorption. For drinking water treatment, although Mg (II) ions would be left in the treated water, its concentration would still far below the WHO limit for Mg (450 mg/L), making flowerlike MgO nanostructures a safe adsorbent for Pb(II) and Cd(II).

Quantitative measurement of the molar amount of Mg (II) released and the amount of Pb(II) or Cd(II) adsorbed indicates a nearly liner relationship (as shown in Figure 6), further confirming the cation exchange between Mg (II) and Pb(II) or Cd(II). Such cation exchange mechanism is different from anion exchange with surface hydroxyl groups. Mg ions are part of the MgO crystal lattice. Exchange between Mg (II) and Pb(II) suggested that Pb(II) cations replace the Mg(II) in the lattice. The overall mechanism is actually a solid-liquid interfacial reaction:

$$MgO + Pb^{2+} = PbO + Mg^{2+}$$

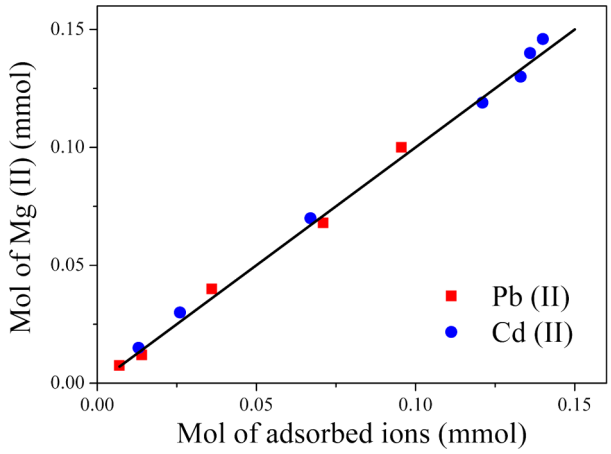

Figure 6. Molar of exchanged Mg (II) vs molar of adsorbed Pb(II) or Cd(II) with flowerlike MgO nanostructures as adsorbents.

The XRD pattern of flowerlike MgO after adsorption of Pb(II) is shown in Figure S2 in the Supporting Information. All the diffraction peaks can be mainly ascribed to MgO and PbO (JCPDS No. 85-1291), suggesting MgO have partially reacted with Pb(II), which verifies the chemical reaction between MgO and Pb(II). In addition, the color of MgO after adsorption Pb(II) was yellow (see Figure S3 in the Supporting Information), which is agreed with the color of PbO, further indicating the chemical reaction. Two small peaks of $Mg(OH)_2$ can be also observed in the XRD pattern of flowerlike MgO after adsorption of Pb(II). This is because MgO can be hydrated to form $Mg(OH)_2$ in water. However, it is just appeared on the very thin surface of MgO. Because there was no $Pb(OH)_2$ formed in the sample after adsorption, confirming the chemical reaction of MgO and Pb(II).

Such mechanism explains the origin of superb capacity of MgO for Pb(II) and Cd(II) observed in this study. For example, the 1980 mg/g removal capacity for Pb(II) represents an about 40 % "conversion" for MgO. It is estimated that for MgO material with 72 m^2/g surface area, about 10 % of the atoms are on the surface.[23] Thus it is likely that the exchange between Mg (II) and Pb(II) occurs at the first few layers of the MgO lattice from the surface. As shown in Figure 4b, the adsorption capacity reaches maximum with an equilibrium concentration of about 100 mg/L. The exchange between Mg (II) and Pb(II) stops when the first few layers of Mg (II) are replaced by Pb(II). PbO may block the further reaction of MgO with Pb(II) after saturated adsorption. SEM image of flowerlike MgO after adsorption Pb(II) (see Figure S4 in the Supporting Information) further shows that the flowerlike morphology was broken with some aggregation.

4. CONCLUSION

In summary, flowerlike MgO nanostructures were produced by a rapid and low cost microwave assisted solvothermal method. They showed superb adsorption properties for heavy metal cations, with maximum capacities of 1980 mg/g and 1500 mg/g for Pb(II) and Cd(II), respectively. A new adsorption mechanism involving cation exchange between magnesium ion and lead or cadmium ion was proposed and confirmed. Because of advantages such as low cost, high surface area, as well as high adsorption capacity, such flowerlike MgO nanostructures were an attractive adsorbent for the removal of both Pb(II) and Cd(II) from drinking water.

■ ASSOCIATED CONTENT

Supporting Information

N_2 adsorption−desorption isotherms of flowerlike MgO nanostructures; XRD pattern, digital photograph, and SEM image of flowerlike MgO after adsorption Pb(II); adsorption properties of flowerlike MgO for Pb(II) and Cd(II) at low concentration; Concentrations of Pb(II), Cd(II), and Mg (II) after adsorption. This material is available free of charge via the Internet at http://pubs.acs.org.

■ AUTHOR INFORMATION

Corresponding Author

*E-mail: wsong@iccas.ac.cn. Tel/Fax: +86-10-62557908.

Notes

The authors declare no competing financial interest.

■ ACKNOWLEDGMENTS

We thank the financial supports from the National Basic Research Program of China (2009CB930400, 2011CB933700), National Natural Science Foundation of China (NSFC 21121063) and the Joint fund from Chinese Academy of Sciences and CSIRO (GJHZ1224).

■ REFERENCES

(1) Fang, Q. L.; Xuan, S. H.; Jiang, W. Q.; Gong, X. L. *Adv. Funct. Mater.* **2011**, *21*, 1902−1909.
(2) Hu, J. S.; Zhong, L. S.; Song, W. G.; Wan, L. J. *Adv. Mater.* **2008**, *20*, 2977−2982.
(3) Zhong, L. S.; Hu, J. S.; Liang, H. P.; Cao, A. M.; Song, W. G.; Wan, L. J. *Adv. Mater.* **2006**, *18*, 2426−2431.
(4) Yantasee, W.; Warner, C. L.; Sangvanich, T.; Addleman, R. S.; Carter, T. G.; Wiacek, R. J.; Fryxell, G. E.; Timchalk, C.; Warner, M. G. *Environ. Sci. Technol.* **2007**, *41*, 5114−5119.
(5) Zhong, L. S.; Hu, J. S.; Cao, A. M.; Liu, Q.; Song, W. G.; Wan, L. J. *Chem. Mater.* **2007**, *19*, 1648−1655.
(6) Cao, C. Y.; Guo, W.; Cui, Z. M.; Song, W. G.; Cai, W. *J. Mater. Chem.* **2010**, *21*, 3204−3209.
(7) Bain, S. W.; Ma, Z.; Cui, Z. M.; Zhang, L. S.; Niu, F.; Song, W. G. *J. Phys. Chem. C* **2008**, *112*, 11340−11344.
(8) Liu, W. Z.; Huang, F.; Wang, Y. J.; Zou, T.; Zheng, J. S.; Lin, Z. *Environ. Sci. Technol.* **2011**, *45*, 1955−1961.
(9) Li, H.; Li, W.; Zhang, Y. J.; Wang, T. S.; Wang, B.; Xu, W.; Jiang, L.; Song, W. G.; Shu, C. Y.; Wang, C. R. *J. Mater. Chem.* **2011**, *21*, 7878−7881.
(10) Wu, Z. X.; Zhao, D. Y. *Chem. Commun.* **2011**, *47*, 3332−3338.
(11) Drisko, G. L.; Luca, V.; Sizgek, E.; Scales, N.; Caruso, R. A. *Langmuir* **2009**, *25*, 5286−5293.
(12) Chen, D. H.; Cao, L.; Huang, F. Z.; Imperia, P.; Cheng, Y. B.; Caruso, R. A. *J. Am. Chem. Soc.* **2010**, *132*, 4438−4444.
(13) Liu, W.; Huang, F.; Liao, Y.; Zhang, J.; Ren, G.; Zhuang, Z.; Zhen, J.; Lin, Z.; Wang, C. *Angew. Chem., Int. Ed.* **2008**, *47*, 5619−5622.
(14) Yu, X. Y.; Luo, T.; Zhang, Y. X.; Jia, Y.; Zhu, B. J.; Fu, X. C.; Liu, J. H.; Huang, X. J. *ACS Appl. Mater. Interfaces* **2011**, *3*, 2585−2593.
(15) Yu, X. Y.; Xu, R. X.; Gao, C.; Luo, T.; Jia, Y.; Liu, J. H.; Huang, X. J. *ACS Appl. Mater. Interfaces* **2012**, *4*, 1954−1962.
(16) Madadrang, C. J.; Kim, H. Y.; Gao, G.; Wang, N.; Zhu, J.; Feng, H.; Gorring, M.; Kasner, M. L.; Hou, S. *ACS Appl. Mater. Interfaces* **2012**, *4*, 1186−1193.
(17) Lee, G.; Chen, C.; Yang, S. T.; Ahn, W. S. *Microporous Mesoporous Mater.* **2010**, *127*, 152−156.
(18) Yu, X. Y.; Luo, T.; Jia, Y.; Zhang, Y. X.; Liu, J. H.; Huang, X. J. *J. Phys. Chem. C* **2011**, *115*, 22242−22250.
(19) Gao, C.; Zhang, W.; Li, H.; Lang, L.; Xu, Z. *Cryst. Growth Des.* **2008**, *8*, 3785−3790.
(20) Sasaki, K.; Fukumoto, N.; Moriyama, S.; Hirajima, T. *J. Hazard. Mater.* **2011**, *191*, 240−248.
(21) Cao, C. Y.; Qu, J.; Yan, W. S.; Zhu, J. F.; Wu, Z. Y.; Song, W. G. *Langmuir* **2012**, *28*, 4573−4579.
(22) Cao, A. M.; Hu, J. S.; Liang, H. P.; Wan, L. J. *Angew. Chem., Int. Ed.* **2005**, *44*, 4391−4395.
(23) Cao, A. M.; Hu, J. S.; Liang, H. P.; Song, W. G.; Wan, L. J.; He, X. L.; Gao, X. G.; Xia, S. H. *J. Phys. Chem. B* **2006**, *110*, 15858−15863.
(24) Chen, D.; Cao, L.; Hanley, T. L.; Caruso, R. A. *Adv. Funct. Mater.* **2012**, *22*, 1966−1970.
(25) Cao, C. Y.; Guo, W.; Cui, Z. M.; Song, W. G.; Cai, W. *J. Mater. Chem.* **2011**, *21*, 3204−3209.
(26) Cao, C. Y.; Cui, Z. M.; Chen, C. Q.; Song, W. G.; Cai, W. *J. Phys. Chem. C* **2010**, *114*, 9865−9870.
(27) Wang, Y.; Wang, G.; Wang, H.; Liang, C.; Cai, W.; Zhang, L. *Chem.—Eur. J.* **2010**, *16*, 3497−3503.
(28) Chen, L. F.; Liang, H. W.; Lu, Y.; Cui, C. H.; Yu, S. H. *Langmuir* **2011**, *27*, 8998−9004.
(29) Qu, J.; Cao, C. Y.; Hong, Y. L.; Chen, C. Q.; Zhu, P. P.; Song, W. G.; Wu, Z. Y. *J. Mater. Chem.* **2012**, *22*, 3562−3567.
(30) Zhang, Y. X.; Jia, Y.; Jin, Z.; Yu, X. Y.; Xu, W. H.; Luo, T.; Zhu, B. J.; Liu, J. H.; Huang, X. J. *CrystEngComm* **2012**, *14*, 3005−3007.
(31) Yu, L.; Zou, R.; Zhang, Z.; Song, G.; Chen, Z.; Yang, J.; Hu, J. *Chem. Commun.* **2011**, *47*, 10719−10721.
(32) Ni, Y.; Mi, K.; Cheng, C.; Xia, J.; Ma, X.; Hong, J. *Chem. Commun.* **2011**, *47*, 5891−5893.